

DISTRIBUTION OF CARBON ATOMS IN IRON-CARBON *fcc* PHASE: AN EXPERIMENTAL AND THEORETICAL STUDY

K. F. Laneri, J. Desimoni

Departamento de Física, Facultad de Ciencias. Exactas, UNLP,

IFLP-CONICET C.C. 67, 1900 La Plata, Argentina

G. J. Zarragoicoechea

Instituto de Física de Líquidos y Sistemas Biológicos

(CICPBA-UNLP) 59 N° 789, C.C. 565, 1900 La Plata, Argentina

A. Fernández-Guillermé

Consejo Nacional de Investigaciones Científicas y Técnicas, Centro

Atómico Bariloche, 8400 Bariloche, Argentina

This paper presents an experimental and theoretical study of the distribution of carbon atoms in the octahedral interstitial sites of the face-centered cubic (*fcc*) phase of the iron-carbon system. The experimental part of the work consists of Mössbauer measurements in Fe-C alloys with up to about 12 atomic percent C, which are interpreted in terms of two alternative models for the distribution of C atoms in the interstitial sites. The theoretical part combines an analysis of the chemical potential of C based on the quasichemical approximation to the statistical mechanics of interstitial solutions, with three-dimensional Monte Carlo simulations. The latter were performed by assuming a gas like mixture of C atoms and vacancies (Va) in the octahedral interstitial sites. The number of C-C, C-Va and Va-Va pairs calculated using Monte Carlo simulations are compared with those given by the quasichemical model. Furthermore, the relative fraction of the various Fe environments were calculated and compared with those extracted from the Mössbauer spectra. The simulations reproduce remarkably well the relative fractions obtained assuming the $\text{Fe}_8\text{C}_{1-y}$ model for Mössbauer spectra, which includes some blocking of the nearest neighbour interstitial sites by a C atom. With the

new experimental and theoretical information obtained in the present study, a critical discussion is reported of the extent to which such blocking effect is accounted for in current thermodynamic models of the Fe-C *fcc* phase.

PACS Codes: 2.70.Uu, 76.

I. INTRODUCTION

The physical properties of the austenite solid solution phase have been studied extensively over the years in connection with, e.g., the assessment and understanding of the phase diagram [1-6], the diffusion controlled [7] and martensitic phase transitions in Fe-C alloys [8]. In austenite the iron atoms are arranged in a close-packed face-centred cubic (*fcc*) lattice, and the C atoms occupy a limited number of the octahedral interstices which are located at the centres and at the mid-points of the edges of the unit cubes, these two positions being crystallographically equivalent (Fig.1) [9]. Accordingly, various models of austenite have been proposed which are based on assuming two sublattices, one for the Fe atoms and the second one for the mixture of carbon atoms (C) and vacant octahedral interstices (Va). The general theme of the present paper is the distribution of the C atoms in the interstitial sites, as revealed by three complementary sources of information, viz., thermodynamic properties, Mössbauer experiments and Monte Carlo simulations.

In the ideal solution model (ISM) for thermodynamic properties of austenite it is assumed that C and Va distribute themselves at random in the octahedral interstitial sites, the amount of which is equal to the number of Fe atoms. On these basis, the thermodynamic activity (a_c) of C in an ideal mixture of N_C carbon atoms with N_{Fe} iron atoms is shown to be proportional to the ratio $y_c/(1 - y_c)$, where $y_c = N_C/N_{Fe}$, and $1 - y_c$ represent the fraction of occupied and of empty interstitial sites, respectively [10-13]. Since the experimental a_c in austenite deviates positively from the ISM, many approaches have been proposed to account for the non-ideal behaviour [14-22]. The reader is referred to ref. [23] for a recent review of the work of most relevance for the present study. In the strict version

of the approach known as the hard-blocking excluded-sites model (HBESM) it is assumed that the presence of a solute atom blocks the occupancy of a certain number (b) of the nearest neighbor interstitial sites (NNIS), so that a site is either blocked or is available for the mixing of C atoms and Va [9, 15, 23]. Further, if the mixing in the non-blocked sites occurs at random, the a_c in austenite becomes proportional to $y_c/[1 - (1 + b)y_c]$ [23]. Frequently, b has been treated as an adjustable parameter, identified with the value to be inserted in the expression for a_c in order to reproduce the experimental data [9,19,22,23]. Alternatively, some theoretical studies have been reported which suggest that b should in fact be treated as composition dependent [18,19]. A different approach will be explored in the present work, which is based on combining two theoretical methods. First, we will adopt the quasi-chemical approximation (QCA) to the statistical mechanics of interstitial solutions [12,24-27]. In the QCA all interstitial sites are available for mixing, but the C atoms are regarded as exerting a repulsive force on each other, so that they enter adjacent interstitial positions less frequently as would be the case if their distribution were random. Thus the QCA will allow us to treat soft-blocking effects in austenite. The key parameters in this treatment are the energies of formation of the C-C and C-Va pairs, which will be accurately determined by analysing a_c data. Secondly, we will perform Monte Carlo (MC) simulations for various values of the N_C/N_{Fe} ratio, using the pair formation energies from the quasi-chemical analysis. In this way, the average distribution of interstitials around a given C atom will be studied as function of composition. In particular, the average number of empty NNIS will be determined for various alloys, and compared with the results of previous studies, as well as with information extracted from Mössbauer experiments.

In the analysis of the Mössbauer spectra of austenite various assumptions about the distribution of C in the octahedral interstitial sites have been proposed [28,29]. In particular, a model has been suggested for dilute solutions in which the 12 NNIS of a C atom are excluded [28]. In this case the C atoms occupy only the centre of the cubes of a structure with the formula Fe_8C_{1-y} , so that three possible environments for Fe atoms, associated to different hyperfine interaction may be distinguished, which are shown schematically in Fig.2,

viz.,

a. Fe atoms without nearest neighbor and next nearest neighbor C atoms, associated to the singlet Γ_{00} .

b. Fe atoms without nearest neighbour but with n next nearest neighbour C atoms ($n = 1 - 4$), ascribed to the singlet Γ_{0n} .

c. Fe atoms with one C atom nearest neighbour but without next nearest C neighbours, related to doublet Γ_{10} .

Alternatively, a model [29] has been proposed in which all the octahedral sites of the *fcc* structure are available for occupation and no assumptions are made on the distribution of the C atoms in the second interstitial shell. The various Fe-C environments involved in this type of model are shown schematically in Fig.3, viz.,

a. Fe atoms without nearest neighbours C atoms, associated to the singlet Γ_0 .

b. Fe atoms with one nearest neighbor C atom, or Fe atoms with two C atoms nearest neighbours at 90° from each other, related to the doublet Γ_1 .

c. Fe atoms with two C atoms placed at opposite nearest sites (180°), ascribed to the doublet Γ_2 .

The purpose of the present paper is to provide new experimental and theoretical information on the distribution of C atoms in the octahedral sites of the austenite phase. The work proceeds as follows. First, Mössbauer experiments are performed on a series of alloys with up to 12 at.%.

II. EXPERIMENTAL

A. Alloys, samples and heat-treatments

Five Fe-C compacted graphite alloys were prepared in a medium frequency induction furnace using the sandwich technique in ladle to treat the liquid metal. The necessary amount of Si, Mg, Ce and Ca was added to obtain compacted graphite morphology. The

final alloy contained 3.40 wt.%C, 2.35 wt.%Si, 0.58 wt.%Mn, 0.04 wt.%Cu, 0.01 wt.%P, and 0.02 wt.%S.

Samples of 20 mm diameter and 3 mm thickness were taken from "Y-shape" blocks (ASTM A-395) cast in sand moulds. Samples S1, S2, S3, S4 and S5 (see below) were annealed at 1173K during 30 minutes, quenched in a salt bath and held at 623K during 1, 3, 4, 5 and 10 minutes respectively. The samples for Mössbauer spectroscopy were prepared by conventional grinding techniques to reduce their thickness down to about 70mm, using diamond paste of 6, 1 and 0.1mm for final polishing.

B. X-ray measurements

X-ray measurements were performed in a Philips PW1710 diffractometer using the monochromatic K_α radiation of Cu, in Bragg Brentano's geometry, with a step mode collection of 0.02, 10s by step, with 2θ ranging from 39° to 98° . The X-ray patterns, presented in Fig.4, were analysed with the Rietveld method [30]. The actual C concentration in the samples was determined by combining the lattice-parameters (a) extracted from the diffraction patterns with the known a versus composition relation for *fcc* Fe-C alloys [28]. The resulting lattice-parameter and the inferred y_c values for the various alloys are listed in Table I.

C. Mössbauer experiments

Mössbauer spectra were taken in a transmission geometry using a ^{57}Co *Rh* source of approximately 5mCi intensity and recorded in a standard 512 channels conventional constant acceleration spectrometer. In order to analyse in detail the austenite pattern, the spectra were taken in the velocity range between - 2 and + 2 mm/s. Velocity calibration was performed against a 12 mm thick α - Fe foil. All isomer shifts were referred to this standard at 298K. The spectra were fitted to Lorentzian line shapes using a non-linear least-squares

program with constraints. For the effective thickness of the samples analysed no Voigt line-shape correction was necessary [31].

The results of the Mössbauer experiments are shown in Fig.5. The central subspectra were associated to austenite, whereas the external lines on the spectra to ferrite/martensite phases [28]. The hyperfine parameters and the relative fractions f_{lm} ($l, m =$ number of C atoms in the first and second coordination shell, respectively) associated to the various Fe environments obtained using the models [28,29] referred to in Sect.I are listed in Table II. Concerning the second model [29], the contribution to the spectra of the doublet Γ_2 associated to Fe sites with two C atoms placed in opposite interstitial sites resulted undetectable by the present technique.

III. THEORETICAL

A. Monte Carlo simulations

The austenite interstitial solid solution is described as a lattice gas of N_C carbon atoms and N_{Va} vacancies, distributed in the $N_C + N_{Va} = N = N_{Fe}$ octahedral interstitial sites of the *fcc* structure (Fig. 1) associated to N_{Fe} iron atoms. The occupancy of the first and second interstitial shell was accounted for in three-dimensional MC simulations to calculate the number n_{ij} ($i, j = C$ or Va) of C-C, C-Va and Va-Va pairs, the relative fractions f_{lm} associated to the different Fe environments, and the number C_{i0} of C atoms having i C atoms in the first interstitial coordination shell and none in the next interstitial shell.

A Fortran 77 routine using the Monte Carlo method, an Ising-type Hamiltonian and periodic boundary conditions was developed. Metropolis method was used to define the probability of the C jumps. A randomly chosen C atom has the probability P to jump to an empty interstitial neighbouring site, also randomly chosen, viz.,

$$P = \begin{cases} \exp[(\varepsilon_{Ti} - \varepsilon_{Tf})/RT] & \text{if } \varepsilon_{Tf} > \varepsilon_{Ti} \\ 1 & \text{if } \varepsilon_{Tf} \leq \varepsilon_{Ti} \end{cases} \quad (1)$$

where ε_{Ti} and ε_{Tf} , are the initial and final total energies, respectively, calculated using the relation $\varepsilon_T = n_{C-C}\Delta\varepsilon$. Here $\Delta\varepsilon = 2 \varepsilon_{C-Va} - \varepsilon_{C-C}$ is the energy of formation of a C-C pair of nearest neighbour C atoms relative to the individual C atoms (see below), n_{C-C} is the number of C-C pairs, ε_{C-C} and ε_{C-Va} are the interaction energies of the C-C and C-Va pairs, respectively, R is the gas constant and T is the temperature in Kelvin. If the atom movement decreases the total energy, the jump is allowed ($P=1$), but if the total energy increases, the jump is allowed with a probability $P = \exp[(\varepsilon_{Ti} - \varepsilon_{Tf})/RT]$. The Fe atoms remain still during the simulation, and their positions were only used to calculate the number of n_{ij} pairs and the relative fractions f_{lm} associated to the different Fe environments.

In order to study the convergence of the results, cells of 4^3 , 6^3 , 8^3 and 10^3 were used. For simulations using cell sizes of 6^3 and higher the n_{ij} and f_{lm} fractions did not vary, hence cells of 864 Fe atoms and the corresponding number of C atoms were employed to decrease the calculation time. For all C concentrations, the equilibrium of the system was attained approximately at three MC steps, where a MC step is defined as N_C attempts of movement of a C atom.

Finally, the occupation of the interstitial sites was characterised using the average number z of empty NNIS, which was calculated from the MC results as follows:

$$z = \frac{\sum_{i=0}^{12} C_{i0}(12 - i)}{\sum_{i=0}^{12} C_{i0}} \quad (2)$$

B. Quasichemical model calculations

The energy of formation of a C-C pair that enters in the MC calculation was determined by analysing experimental a_c data in terms of the QCA to the statistical mechanics of the Fe-C solutions developed by Bhadeshia [27]. This formalism yields for the activity a_c

$$a_c = \frac{y_c}{1 - y_c} \exp\left[\frac{\Delta G_c}{RT}\right] \left\{ \left(\frac{y_c}{1 - y_c} \right)^2 \left(\frac{1 - y_c - \frac{\bar{\lambda}}{N_{Va}}}{1 - y_c} \right) \right\}^{\frac{-z}{2}} \exp\left[\frac{-Z\Delta\varepsilon}{2RT}\right] \quad (3)$$

where Z (=12) is the number of NNIS, and ΔG_c is the Gibbs energy of C in austenite relative to graphite. The value of the parameter $\bar{\lambda}$ that minimise the Gibbs energy is:

$$\bar{\lambda} = \frac{N_{Va}}{2\sigma} \left\{ 1 - \left[1 - 4\sigma y_c (1 - y_c)^{\frac{1}{2}} \right] \right\}$$

with

$$\sigma = 1 - \exp \left[\frac{-\Delta\varepsilon}{RT} \right]$$

A linear approximation of Eq.3, appropriate for describing the dilute solution range was fitted to carbon activity data measured at 1423K [22]. A least-squares fit of the equation:

$$RT \ln \left[a_c \frac{1 - y_c}{y_c} \right] = y_c Z \Delta\varepsilon + \Delta G_c$$

which is shown in Fig.6 yielded $\Delta G_c=4451_{25}$ cal/mol, and $\Delta\varepsilon=1492_{39}$ cal/mol. This one was adopted in the MC simulations.

The number of pairs n_{ij} calculated for $0 < y_c < 1$ using the quasichemical formalism (Table III) are plotted in Fig. 7 using lines. For comparison the n_{ij} determined in the MC calculations using $\Delta\varepsilon = 1492$ cal/mol are plotted using symbols. The inset there gives a comparison for the composition range corresponding to the experimental solubility of C in austenite, viz., $y_c < 0.1$. There is a very good agreement between the QCA and the MC predictions for n_{ij} , which encourages a discussion of the MC results for the relative fractions f_{lm} of the various Fe environments, as functions of y_c .

IV. DISCUSSION

A. Monte Carlo versus Mössbauer results

The MC results for the f_{lm} as functions of y_c are plotted in Fig. 8. According to the present simulations the main contributions to the Mössbauer spectra originate in the Fe environments without C atoms in the first interstitial shell (f_{00} and f_{0n}). Next in importance is the contribution of environments with one C atom in the first interstitial shell and none

in the second (f_{10}). Further, the simulations show that the contribution of Fe atoms having the first and second interstitial shells occupied (f_{nm}) is not negligible, which indicates that this kind of Fe environments should be accounted for in fitting Mössbauer spectra. Figure 8 also demonstrates that the relative fraction associated to Fe atoms with more than one C atom in the first interstitial shell and without C atoms in the second shell (f_{n0}) is negligible. This result contradicts the assumption of one of the models [29] developed to interpret the Mössbauer pattern of the austenite, which was reviewed in Sect.I. In fact, we find that the contribution of Fe environments with two C atoms either at 90° or 180° is negligible.

In order to compare the MC results with the results of analysing the present Mössbauer spectra (Table II), the relative fractions f_{00} and the sum $f_0 = f_{00} + f_{0n}$ were chosen as the key quantities in the $\text{Fe}_8\text{C}_{1-y}$ model [28] and the random model [29], respectively. The reason for this choice is that Fe environment with C atoms in the first and the second interstitial shells have not been considered by any of the models proposed to reproduce the Mössbauer spectra [28,29]. Moreover, we have also shown that the fraction of Fe environments with two C atoms in the first shell is negligible according to MC results. Hence, the only fractions that can be determined without ambiguity for these models are f_{00} and f_0 , respectively.

A comparison between the f_{00} and f_0 versus composition values extracted from the Mössbauer spectra (open symbols) and the MC simulations (filled symbols) is presented in Fig. 9. According to Fig. 9 the "random model" underestimates significantly the contribution of the Fe environments without nearest neighbour C atoms. This suggests that in this composition range, some blocking effect of the NNIS in austenite should be accounted for. In agreement with this expectation, the MC results fit remarkably well with the f_{00} values extracted from Mössbauer experiments when the $\text{Fe}_8\text{C}_{1-y}$ model is adopted, i.e., the model including some blocking effect of the interstitial sites.

Finally, MC simulations have been reported previously [32] which are based on extracting from Mössbauer measurements a weak C-C repulsion in the first coordination shell ($w_1 = 830$ cal/mol) and a stronger one ($w_2 = 1730$ cal/mol) in the second shell. Such calculations were interpreted [29,32] as indications that the $\text{Fe}_8\text{C}_{1-y}$ model is not adequate to represent

the austenite phase. Similar results ($w_1 = 830$ cal/mol) were arrived at in ref. [29] by assuming that pairs of C atoms can occupy the first interstitial shell either at 90° or at 180° . The present MC results, based on energies extracted from thermodynamic data, do not support these results.

B. Account of blocking effects

In Fig. 10 the average number of empty NNIS z obtained from the MC simulations is plotted as function of y_c (symbols). The z values corresponding to the composition of the present experimental alloys are plotted using empty symbols. The dashed line in this graphic refers to the z value corresponding to a random mixture, viz., $z = 12(1 - y_c)$. The empty symbols in Fig.10 indicate that already in alloys with $y_c = 0.05$ the NNIS of the C atoms are, on the average, less occupied than in a random mixture. This fact is in qualitative agreement with the ideas behind the excluded-sites model, which motivates the following analysis of the blocking effects in models for a_c in austenite.

It has recently been pointed out [23] that in a strict hard-blocking model, empty sites must be interpreted as blocked sites. This implies that the b parameter of the HBESM (Sect.I) should be considered as equal to z (Fig.10). Two consequences of such interpretation will be discussed. The first consequence is that the MC results in Fig.10 cannot be represented using the HBESM unless the b parameter is allowed to vary with composition. In qualitative agreement with this, Oates et al. [21] interpreted their own z values from MC calculations as a composition dependent b parameter, decreasing with the increase in the C content. However, the excluded sites model does not explain the composition dependence of b , which has stimulated some attempts to improve the simple picture by invoking, e.g., overlapping of the sites excluded by different interstitial atoms [17,19,21,23]. The second consequence of the current [23] interpretation of the hard-blocking is that Fig. 10 yields $b (=z) > 10$ in the composition range $y_c < 0.2$. However, these values cannot be reconciled with those extracted from experimental a_c data. The latter are integral and non-integral b

values falling in the range $3 < b < 5$ [9,19,22,23].

In view of these facts we conclude that the strict form of the excluded-sites model (Sect.I) does not seem able to account for the present blocking effects by using the same b values which are known to reproduce the experimental a_c data. It is also evident that a more realistic account of such effects would require abandoning the one-parameter formula for a_c , i.e., what has been considered as the main advantage of the HBESM [23].

V. SUMMARY AND CONCLUDING REMARKS

In the present study the energy parameters describing the interstitial solution of C in the *fcc* phase of Fe have been obtained by analyzing experimental thermodynamic data in terms of the quasichemical approximation. These parameters have been used as input information in Monte Carlo simulations, and various key quantities have been obtained. In particular, the composition dependence of various f_{ij} ratios, describing the relative weight of the various Fe configurations contributing to the Mössbauer spectra of Fe-C austenite, have been predicted and compared with those derived by modelling the Mössbauer spectra. In this way, two alternative models [28,29] for the contribution of the Fe environments have been tested. The present comparison between Mössbauer and theoretical results indicates that a description similar to the Fe_8C structure [28] should be preferred for the Fe-C austenite phase. Such a model [28] is usually associated to the blocking of some of the nearest neighbour interstitial sites by a C atom. However, the present results cannot be accounted for by the simplest hard-blocking excluded sites model, often used to provide a one-parameter formula for the activity of C in austenite. We believe that the picture of blocking effects in austenite emerging from the present study should be useful in further attempts to refine the current models for thermodynamics of interstitial solutions.

ACKNOWLEDGMENTS

This work was partially supported by Consejo Nacional de Investigaciones Científicas y Técnicas (CONICET), PICT 1277, PICT 034517 and PICT-99-03-6507 of the Agencia

Nacional de Promoción Científica y Tecnológica (ANPCyT). G. J. Z. is member of Carrera del investigador CICPBA.

REFERENCES

- [1] L. S. Darken and R. W. Gurry, "Physical Chemistry of Metals", McGraw Hill, New York, 1953.
- [2] M. Benz and J. Elliott, Trans. AIME **221**, 323 (1961).
- [3] H. Harvig, Jernkontor. Ann. **155**, 157 (1971).
- [4] J. Chipman, Met. Trans. **3**, 55 (1972) .
- [5] J. Agren, Met. Trans. **10A**, 1847 (1979).
- [6] P. Gustafson, Scand.Journ.Met. **14**, 259 (1985).
- [7] "Decomposition of Austenite by Diffusional Processes", V. F. Zackay and H. I. Aaronson, editors. Interscience Publishers, New York, 1962.
- [8] "Martensite", G. B. Olson and W. S. Owen editors. American Society for Metals International, 1992.
- [9] L. Kaufman, S. V. Radcliffe and M. Cohen in ref[7], p.313.
- [10] J. R. Lacher, Proceed. Royal Society (London) Ser.A **161**, 525 (1937) .
- [11] J. R. Lacher, Proceed. Camb. Phil. Soc. **33**, 518 (1937).
- [12] R. Fowler and E.A.Guggenheim, "Statistical Thermodynamics", Cambridge Univ. Press, Cambridge, 1956.
- [13] R. W. Gurney, "Introduction to Statistical Thermodynamics", McGraw Hill, New York, 1949.
- [14] R. B. McLellan, in "Phase Stability in Metals and Alloys", P. S. Rundman, J. Stringer and R. I. Jaffee, editors. McGraw Hill Co, New York, 1968.
- [15] R. Speiser and J. W. Spretnak, Trans. ASM **47**, 493 (1955).
- [16] K. A. Moon, Trans.AIME **227**, 1116 (1963) .
- [17] R. B .McLellan, T. L. Garrard, S. J. Horowitz and J. A. Sprague, Trans AIME **239**, 528 (1967).
- [18] P. T. Gallagher, J. A. Lambert and W. A. Oates, Trans.AIME **245**, 887(1969).
- [19] H. M. Lee, Metall.Trans. **5**, 787 (1974).

- [20] M. Hillert and L-I. Staffansson, *Acta Chem.Scand.* **24**, 3618 (1970).
- [21] W. A. Oates and T. B. Flanagan, *Journ.Mat.Science* **16**, 3235 (1981).
- [22] S. Ban-ya, J. F. Elliott, and J. Chipman, *Trans. AIME* **245**, 1199 (1969).
- [23] M. Hillert, *Zeits. Metallkde*, **90**, 60 (1999).
- [24] E. A. Guggenheim, "Mixtures", Oxford Univeristy Press, 1952.
- [25] L. S. Darken and R. P. Smith, *Journ.Amer.Chem.Soc.* **68**, 1172 (1946).
- [26] R. B. Mc Lellan and W. W. Dunn, *J. Phys. Chem. Solids* **30**, 2631 (1969).
- [27] H.K.D.H. Badheshia, *Mater.Sci. and Technology* **14**, 273 (1998).
- [28] O.N.C.Uwakweh, J.P.Bauer and J.M.Génin, *Metall. Trans.* **A21** 589 (1990).
- [29] K. Oda, H. Fujimura, H. Ino, *J. Phys.:Condens Matter* **6**, 679 (1994).
- [30] R. A. Young, in: *The Rietveld method*, (International Union of Crystallography, Oxford, University Press, 1993).
- [31] D. G. Rancourt, A. M. Mc Donald, A. E. Lalonde and J. Y. Ping: *American Mineralogist* **78**, 1(1993).
- [32] A. L. Sozinov, A.G. Balanyuk and V.G. Gavriljuk, *Acta Mater.* **45**, 225 (1997).

FIGURE CAPTIONS

Figure 1: Interstitial sites of the austenite *fcc* phase. a) \blacksquare : C atom, b) \bullet : Vacancy, c) dotted line: C-Va pair, d) solid line: Va-Va pair and e) dashed line: C-C pair. Fe atoms are placed in the corners of the cube and in the face centres.

Figure 2: Fe environments in the $\text{Fe}_8\text{C}_{1-y}$ model [28]. Filled and open circles correspond to C and Fe atoms, respectively.

Figure 3: Fe environments in the random model [29]. Filled and open circles correspond to C and Fe atoms, respectively.

Figure 4: X-Ray diffractograms of samples S1 to S5. The bottom bar diagrams indicate from top to bottom: ferrite, austenite, martensite and C graphite.

Figure 5: Mössbauer spectra recorded for samples S1 to S5.

Figure 6: Linear fit for activity data of ref.[22]. The values $\Delta\varepsilon = 1492_{39}$ cal/mol and $\Delta G_c = 4451_{25}$ cal/mol were determined.

Figure 7: The number n_{ij} ($i, j = \text{C or Va}$) of pairs C-C, C-Va and Va-Va. Squares, triangles and circles represent Va-Va, C-C and C-Va pairs respectively, obtained from Monte Carlo simulations using $\Delta\varepsilon=1492$ cal/mol. a) dash-dotted line: Va-Va, b) dashed line: C-C pairs and c) dotted line: C-Va pairs, calculated using the quasichemical model with the same $\Delta\varepsilon$ value. The inset gives a comparison for the composition range corresponding to the experimental solubility of C in austenite, viz., $y_c < 0.1$.

Figure 8: The relative fractions f_{lm} ($l, m =$ number of C atoms in the first and second coordination shell, respectively) associated to the various Fe environments obtained using Monte Carlo simulations, as functions of C content.

Figure 9: The relative fractions f_{00} (circles) and f_0 (diamonds) associated to the various Fe environments obtained from Mössbauer data (open symbols) using the models [28,29] referred to in Sect.I, compared with results from Monte Carlo simulations (filled symbols).

Figure 10: The average number z of empty nearest neighbour interstitial sites of a C atom in austenite calculated as a function of composition using Monte Carlo simulations.

TABLE CAPTIONS

Table I: Lattice parameter (a) determined from the diffractograms using Rietveld [30] and corresponding to the samples S1, S2, S3, S4 and S5. The C content was determined using the empirical relation of ref.28.

Table II: Hyperfine parameters and relative fractions of the different Fe environments found in austenite using the models of refs. 28 and 29.

Table III: Pair interaction energy and number of n_{ij} pairs in the austenite phase obtained using the quasichemical model [27].

Table I

Sample	Cell constant a (\AA)	y_c
S1	3.610 ₁	0.052 ₁
S2	3.626 ₁	0.076 ₁
S3	3.628 ₁	0.079 ₁
S4	3.630 ₁	0.082 ₁
S5	3.632 ₁	0.086 ₁

Table II

Sample	Γ_{00}		Γ_{0n}		Γ_{10}			Γ_1			Γ_0	
	δ <i>mm/s</i>	f_{00} %	δ <i>mm/s</i>	f_{0n} %	Δ <i>mm/s</i>	δ <i>mm/s</i>	f_{10} %	Δ <i>mm/s</i>	δ <i>mm/s</i>	f_1 %	δ <i>mm/s</i>	f_0 %
S1	-0.1	43 ₁	0.05 ₁	16 ₁	0.66 ₁	-0.01 ₁	41 ₂	0.61 ₁	-0.01 ₁	43 ₂	-0.07 ₁	57 ₁
S2	-0.1	33 ₁	0.05 ₁	23 ₁	0.67 ₁	0.01 ₁	44 ₂	0.62 ₁	0.01 ₁	48 ₁	-0.05 ₁	52 ₁
S3	-0.1	29 ₇	0.06 ₁	23 ₁	0.67 ₁	0.01 ₁	48 ₃	0.63 ₁	0.02 ₁	51 ₁	-0.04 ₁	49 ₁
S4	-0.1	27 ₁	0.06 ₁	21 ₁	0.67 ₁	0.01 ₁	52 ₂	0.63 ₁	0.02 ₁	50 ₁	-0.04 ₁	50 ₁
S5	-0.1	24 ₂	0.05 ₁	25 ₂	0.67 ₁	0.01 ₁	51 ₃	0.63 ₁	0.02 ₁	56 ₁	-0.03 ₁	44 ₁

Table III

Kind of pair	Number of pairs (n_{ij})	Energy per pair
Va-Va	$n_{V_a-V_a} = \frac{1}{2} Z N (1-y_c-\lambda)$	0
C-Va+Va-C	$n_{C-V_a} = Z N \lambda$	ε_{C-V_a}
C-C	$n_{C-C} = \frac{1}{2} Z N (y_c-\lambda)$	ε_{C-C}

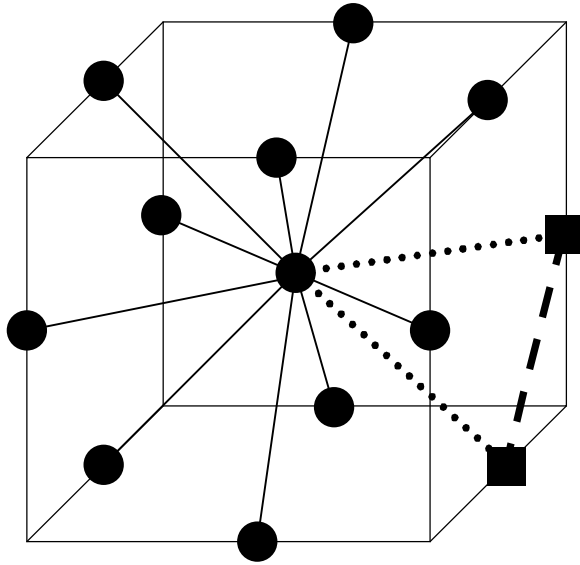
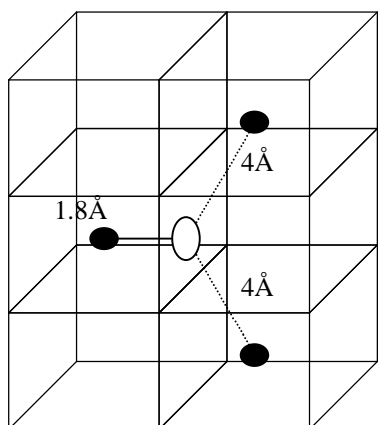
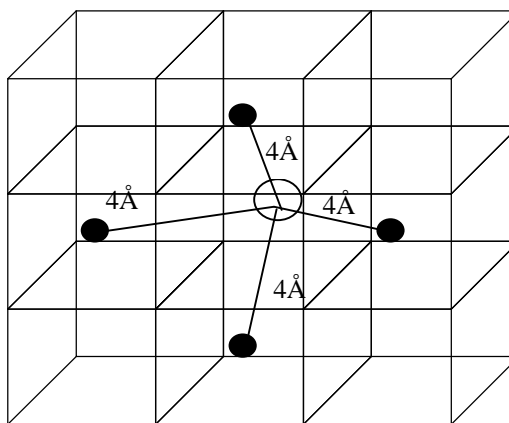


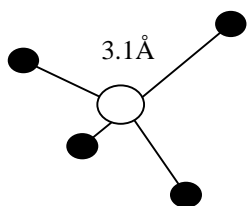
Figure 1, K. Laneri, PRB



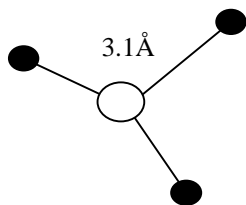
Γ_{10}



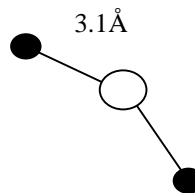
Γ_{00}



Γ_{04}

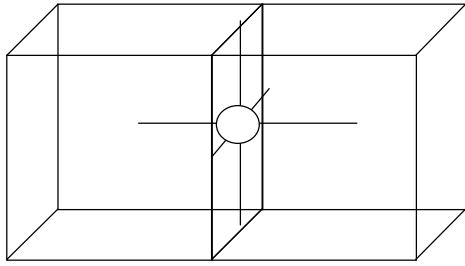


Γ_{03}

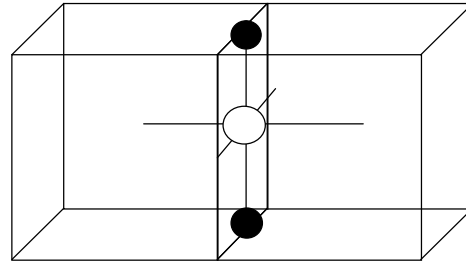


Γ_{02}

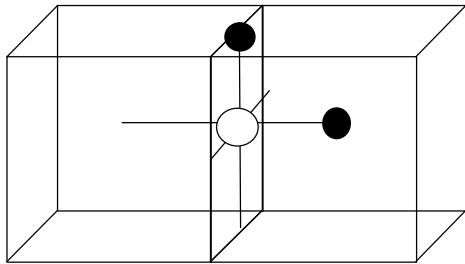
Figure 2, K. Laneri, PRB



Γ_0



Γ_2



Γ_1

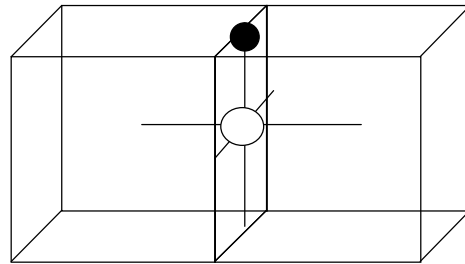


Figure 3, K. Laneri, PRB

intensity (a.u)

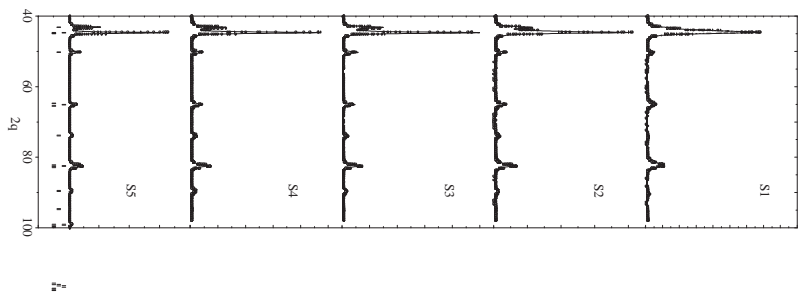


Figure 4, K. Laneri, PRB

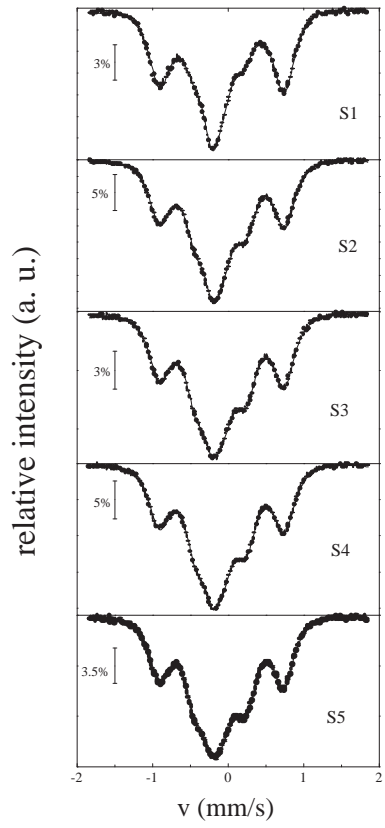


Figure 5. K. Laneri, PRB

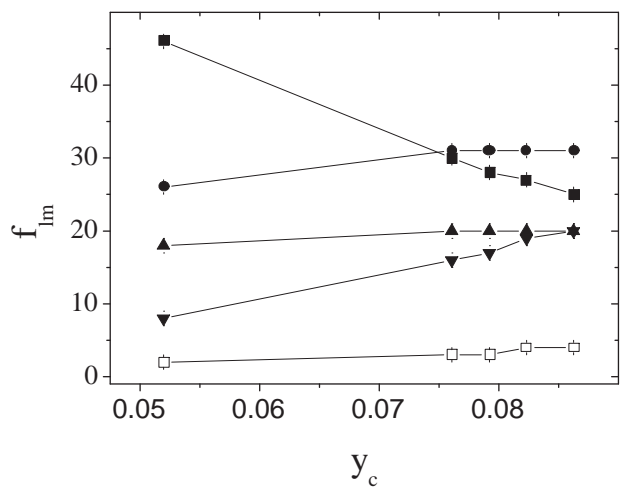


Figure 8, K. Laneri, PRB

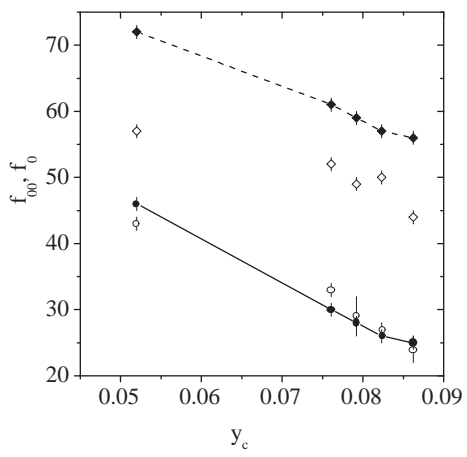


Figure 9, K. Laneri, PRB

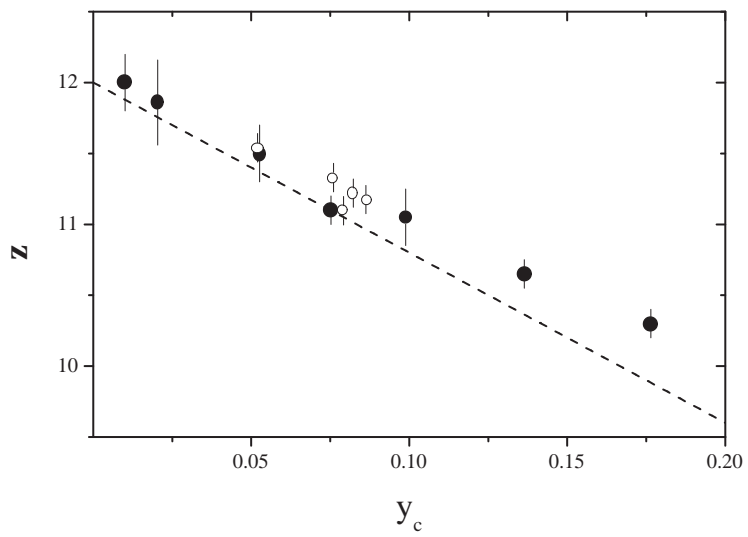


Figure 10, K. Laneri, PRB